Impact of Dielectric Separation on Transition Point and Accessible Flow Enthalpy of Inductive Plasmas

Ashley R. Chadwick [1], Georg Herdrich [2], Min Kwan Kim [1], Bassam Dally [1], Johanna Hertel [2]
[1] University of Adelaide, North Terrace, Adelaide, 5005, Australia, ashley.chadwick@adelaide.edu.au
[2] Institute for Space Systems, University of Stuttgart, Pfaffenwaldring 29, 70569, Stuttgart, Germany, chadwick@irs.uni-stuttgart.de

KEYWORDS

Electric propulsion; Inductive propulsion; Inductive transition

ABSTRACT

In order to develop inductive electric propulsion systems towards flight-ready status, an investigation into the influence of the dielectric separation between plasma and inductive coil has been conducted. This was completed by varying the wall thickness of the thruster discharge tube. The investigation assessed discharges of argon and an argon-nitrogen mixture. Additionally, results of a similar investigation utilising air have been included for comparison. The sum of these investigations showed two contrasting trends. The argon condition exhibited a preference for thicker walls, with transitions to the higher inductive regime occurring at lower input powers with increasing wall thickness. Results for Ar:N_2 and air showed the opposite, with system thermal power increasing with decreasing wall thicknesses. This behaviour has been proposed to include contributions of both the mechanical dielectric separation caused by the choice of chamber wall thickness, and the gasdynamic dielectric separation owing to the discharge thermal boundary layer.

1. INTRODUCTION

With near-future targets for the development of high-power electric propulsion (EP) being introduced [1], the need for new solutions to long-standing or imminent limitations is evident. Despite their high performance, most conventional EP systems lend themselves to preferable operation with noble gases, relying on the low ionisation energy to produce a relatively high flux of energetic particles for thrust generation. However, these gases are inherently rare in the natural environment, resulting in prohibitively high production costs when considering such gases for large-scale propulsion purposes [2]. Many of the current EP systems are subject to ongoing investigations into the implementation of more naturally occurring gases as propellant substitutes, though these gases are often at cross-purposes with the respective thruster acceleration mechanisms. Conventional systems utilising more natural, or 'alternative' propellants usually suffer from both reduced thrust, due to the greater input energy required to generate ions, and corrosion of the electrode/accelerating grid arrangement resulting from contact with aggressive species such as oxygen [3–5].

One branch which does not share these disadvantages is Inductive Electric Propulsion (IEP). IEPs separate their excitation mechanism (an inductive coil or antenna) from the working fluid by means of a dielectric containment vessel, thus allowing the use of corrosive species without adverse damage to critical components [6]. This separation also affords IEPs a wide variety of available propellants, including naturally-occurring compounds such as oxygen and CO_2. Such systems are thus ideally-suited towards missions requiring large propellant supplies, such as satellite orbit-raising or cis-lunar cargo transport operations, making full advantage of their long lifetime (due to the resultant plasma being contained within a chemically-inert vessel) and their ability to be scaled according to a given set of mission objectives (without the need for clustering, which in its execution requires additional propulsion subsystem mass).

Due to the greatly varying chemical properties of available propellants for IEP systems, each exhibits its own behaviour in the context of thrust generation which must be understood before they are implemented into a mission-capable

system. This paper focuses on the impact of the dielectric separation between plasma and inductive coil for a number of gases and gas mixtures, expanding on previously published studies by broadening the number of gases analysed and presenting previously unexpected, contrary behaviour. In particular the work focuses on the separation's influence on the transition point between capacitive and inductive discharge regimes and the accessible enthalpy of the resultant plasma flow. Through analysing a number of chemically diverse propellant configurations, an assessment is made to help clarify why different compositions show preferences towards a particular dielectric chamber wall thickness.

2. INDUCTIVE ENERGY COUPLING

In order to effectively utilise gases as propellant within an IEP, an inductive discharge must be reached, bypassing the capacitive regime which is known to occur at lower powers and discharge pressures [6–9]. The inductive regime exhibits a far more effective energy coupling between the generator coil and the plasma [6, 10], thus providing a more energetic flow for thrust generation either through expulsion of the hot gas or dedicated acceleration of the charged particles.

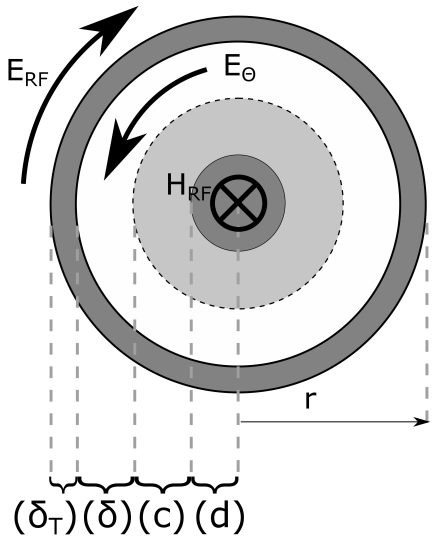

Figure 1: Inductive discharge cross-section

Once the inductive mode has been reached, it displays a very characteristic form as seen in Figure 1, where δ_T is the thermal boundary layer, δ is the skin depth, c is the diffusion zone and d is the cold core flow. In this diagram E_{RF} is the azimuthal electric field generated by the coil current, H_{RF} is its resultant magnetic field, and E_Θ is the opposing electric field generated within the plasma. However, the conditions under which the transition from capacitive to inductive operation occurs is subject to a number of thermodynamic and electromagnetic influences. The instigation of the inductive discharge is reliant on the coil magnetic field exerting sufficient influence over the working fluid volume to sustain the azimuthal electric field, E_Θ, which is itself generated by the motion of charged species (chiefly electrons) within the discharge volume. Therefore the magnetic field must supply sufficient energy to ionise the gas by means of Ohmic (collisional) heating to reach the inductive mode.

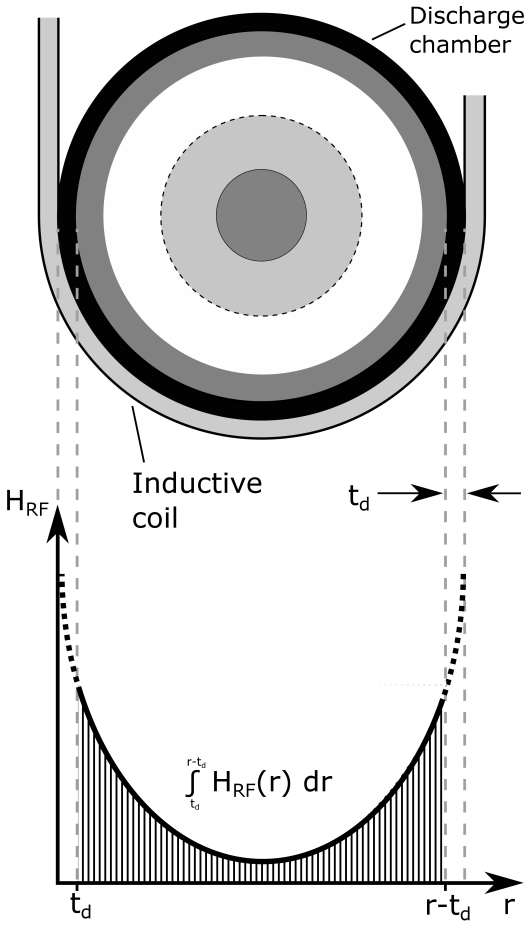

Figure 2: Impact of discharge chamber dielectric wall thickness on incident magnetic field strength

The net magnetic field to which the propellant is exposed is heavily dependent on the distance between the coil surface and the gas, dictated primarily by the thickness of the dielectric discharge chamber. As illustrated in Figure 2, the strength of the incident magnetic field decreases rapidly with increasing distance from the coil surface. Therefore the greater the discharge chamber wall thickness, termed here t_d, the lower the magnitude of the net magnetic field to which the working gas is exposed. While measurements within the discharge chamber during operation are difficult, this variation in net magnetic field can be inferred through observations of the discharge transition point and the resultant sudden increases in both discharge tube and jet thermal power (as discussed in Section 3.).

3. EXPERIMENTAL FACILITY

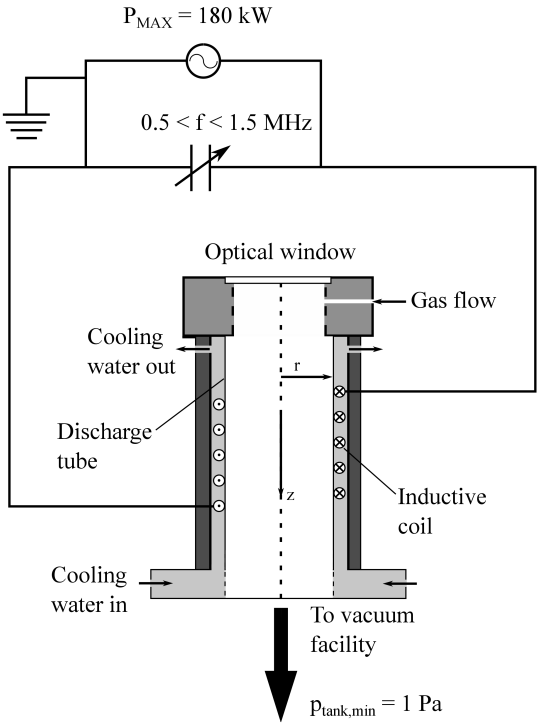

Figure 3: IPG7 apparatus

The results presented in this paper include previous work published by Nawaz and Herdich (2009). While the experimental setup for these results is slightly different to that used to produce the original results for this paper, the two systems represent different generations of the Inductive Plasma Generator (IPG) program at the Institute for Space System (IRS) and thus their behaviours with respect to variations in discharge chamber wall thickness may be considered as equivalent.
Measurements published previously were performed using the IPG3 system, while those produced for the purpose of this paper utilise its successor, IPG7. The two differ only in their mechanical construction and a slight modification to their geometry (a change in discharge chamber outer diameter from 88 mm to 90 mm and a decrease in chamber length from 300 mm to 285 mm), with the associated power supply, resonant circuit, and other supporting systems remaining unchanged. A schematic of the IPG7 apparatus is seen in Figure 3, with images of the generator and jet during capacitive and inductive operation shown in Figures 4 and 5 respectively.

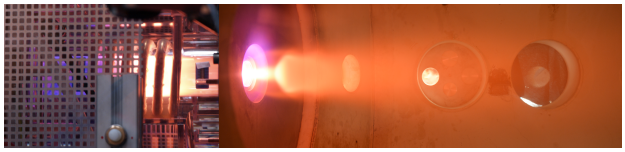

Figure 4: Capacitive discharge (generator and jet), nitrogen

Figure 5: Inductive discharge (generator and jet), nitrogen

The IPG7 is a propellant-flexible radio-frequency (RF) plasma generator, operating at a maximum electrical input power of 180 kW. A set of 7 capacitors (each with a capacitance of 6 nF $\pm$ 20 %) may be used to moderate the generator (capacitive) driving frequency between 0.5 and 1.5 MHz. For this experiment, 5 capacitors were connected, yielding an operational frequency of approximately 580 kHz. The generator is connected to a 9.4 m^3 vacuum tank, capable of reaching pressures of less than 1 Pa without propellant flow. During operation, the high propellant flow rates (in the order of 1-5 g/s) tank pressures typically reach 10-30 Pa.

The gases used within this study were argon

and a mixture of argon and nitrogen, while results extracted from previous publications focused on air [10]. The combination of these gases covers both the monatomic and diatomic propellant classes, providing useful information on their respective preferences. Discharge chamber wall thicknesses investigated within this work were between 2.2 and 4.0 mm. Thicknesses from previous studies covered a range from 1.25 to 2.3 mm. It should also be noted that experiments from [10] were conducted using a 4-capacitor arrangement, yielding a slightly higher operating frequency ($\approx$ 640 kHz) than that implemented in this campaign. However, given that the variation is small and the trends with respect to wall thickness largely decoupled from the operating frequency, the behaviour may be compared without concerns over compatibility.

Measurements of the discharge transition point, jet thermal power, and discharge chamber thermal power were performed using a combination of the cavity calorimeter [6] and thermometers integrated into the IPG cooling circuit. An image of the calorimeter is available in Figure 6.

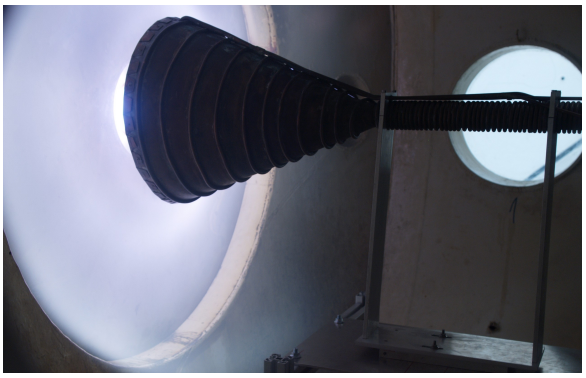

Figure 6: Cavity calorimeter during operation with argon

The IPG cooling circuit and calorimeter measure thermal power in the discharge chamber and thruster jet respectively, and may be combined to determine the performance of a particular propellant.
Given the electrothermal nature of the system, the proportion of input electrical power converted to thermal power is of particular interest, described as:

$$\eta_{th} = \frac{P_{pl} + \dot{Q}_{RF}}{P_A} \tag{1}$$

where P_{pl} is the plasma jet thermal power, $\dot{Q}_{RF}$ is the cooling power of the discharge chamber, and P_A is the electrical input power at the power supply anode. However, when considering this test platform in a thrust application, it is worth determining how much of the thermal power generated by the discharge is conveyed into the thruster jet. This is termed the effective thermal efficiency ($\eta_{th,eff}$), given by:

$$\eta_{th,eff} = \frac{P_{pl}}{P_{pl} + \dot{Q}_{RF}} \tag{2}$$

Analyses of the flow thermal power also allow the impact of discharge regime transitions on thruster performance to be assessed.

Given the different propellant configurations compared within this paper, it is useful to assess their volumetric quantities so as to account for their respective chemical properties. A comparison is provided in Table 1.

Table 1: Propellant volumetric comparison

Propellant	**Original units**	**Molar mass [kg/mol]**	**Equivalent flow, Ar [ln/min]**
Ar	100 ln/min	40	100
Ar:N_2	67:41 ln/min	35	124
Air [10]	2.75 g/s	29	178

This comparison assists in identifying the magnitude of influences in the experimental results and their possible sources.

4. RESULTS

Figures 7 and 8 display the thermal (calorimetric) powers measured within this test campaign.
As can be seen, the influence of wall thickness is substantial on the pure argon flow, with total thermal powers both in the discharge chamber and in the resultant jet increasing with increasing wall thickness. The transition point at which the inductive conditions are reached is also reduced with increasing wall thickness, inferring an improved interactivity between the inductive coil and the gas flow.
Results for the argon-nitrogen mix are, though less extreme in their variation, substantially different from those of pure argon. In these serials thermal

power shows a slight decrease with increasing wall thickness, with all three variations keeping to similar transition points. This implies that, though slight, the preference for this blend tends towards thinner tubes. A further point of detachment between the two is the difference in magnitude of the powers measured, with calorimetric power for the 3.0 mm condition almost a factor of 10 greater in Ar:N_2 than pure Ar. This increase is significantly more than that which could be attributed to the equivalent volumetric flow discussed in Table 1.

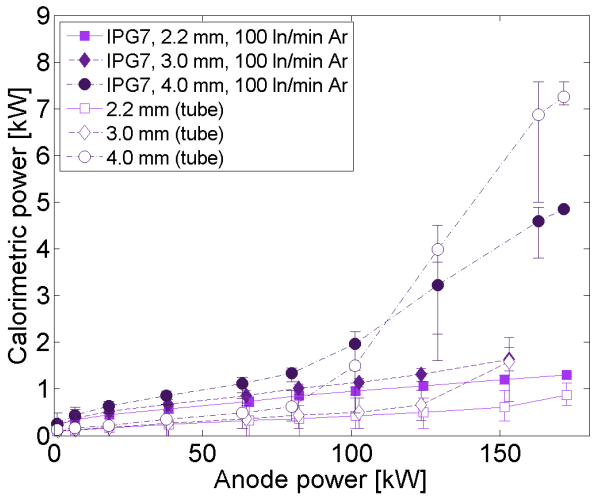

Figure 7: Calorimetric thermal power for the jet and discharge chamber (tube) utilising argon

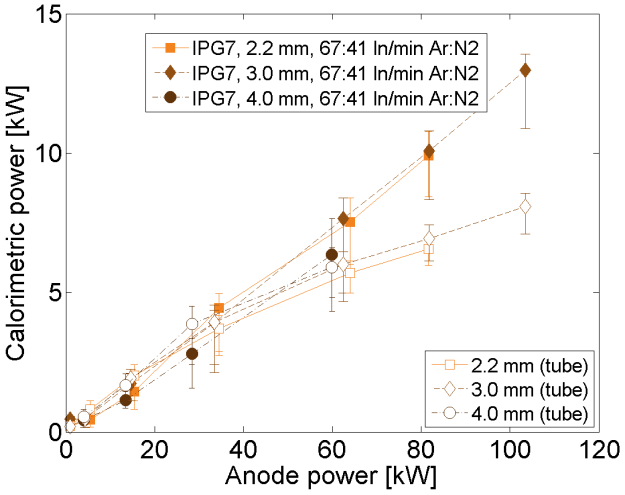

Figure 8: Calorimetric thermal power for the jet and discharge chamber (tube) utilising the argon-nitrogen blend

In comparing these results to previously explored conditions with air (Figure 9), it can be seen that the introduction of nitrogen into the argon flow produces similar trends with respect to wall thickness variation, while operation with a pure argon flow yields a completely inverse behaviour.

A comparison of visible radiation emitted by the two conditions, as seen in Figure 10, reveals that the Ar:N_2 blend has more in common (visually) with a pure nitrogen flow than an equivalent argon flow. Hence the dominance of nitrogen order of magnitude thermal energies is not unexpected.

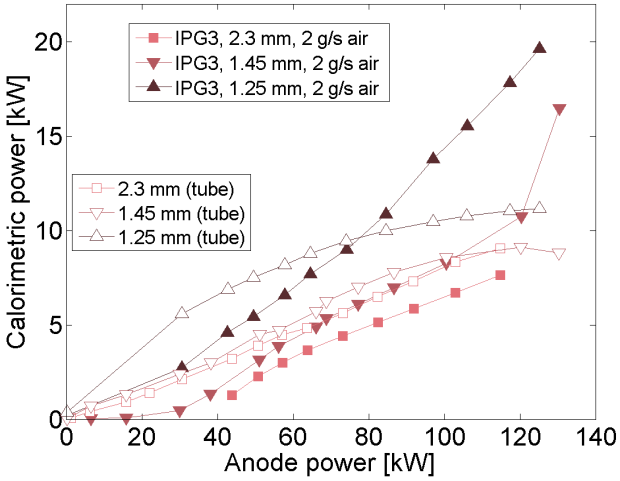

Figure 9: Calorimetric thermal power for the jet and discharge chamber (tube) utilising air (adapted from [10])

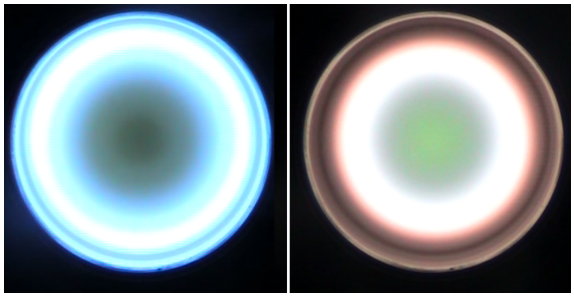

Figure 10: Chamber discharge cross-sections for Ar 171 kW (left) and Ar:N_2 103 kW (right)

It is therefore proposed that the opposing trends of pure Ar and Ar:N_2 are linked to the nature of chemical reactions present within the discharge, providing an additional aspect to the effective dielectric separation of plasma and coil. A more thorough discussion of this concept conducted in Section 5.

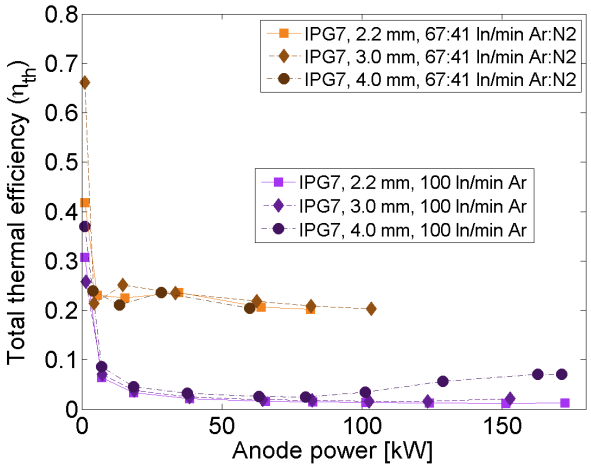

Figure 11: Total thermal efficiency for argon and argon-nitrogen blend

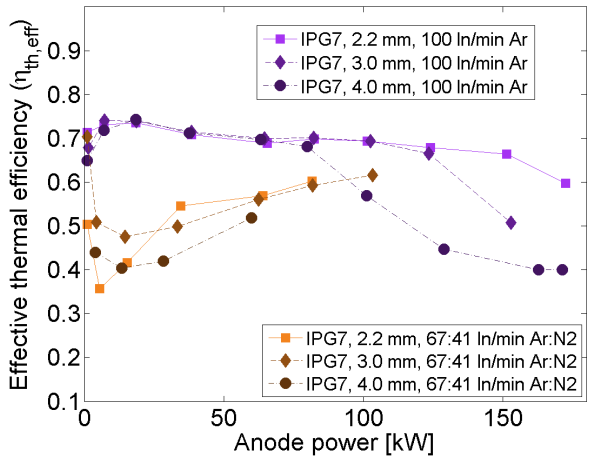

Figure 12: Effective thermal efficiency for argon and argon-nitrogen blend

Figures 11 and 12 display the total and effective thermal efficiencies of the system respectively for the Ar and Ar:N_2 conditions. As is expected, thermal efficiency for the argon flow remains low except in the case of the 4.0 mm condition where sustained operation in the higher-enthalpy discharge mode (as opposed to short durations at the end of the power scale for 2.2 and 3.0 mm) causes a slight increase in the total thermal efficiency. However, an analysis of the effective efficiency shows that this increase is dominated by thermal power within the discharge chamber rather than the jet and hence the usable thermal power for thrust applications actually decreases. This decrease is of course assuming purely electrothermal thrust, with acceleration mechanisms such as magnetic nozzles seen as a way to make use of the greater ionisation degrees associated with such conditions. These however are considered purely anecdotally within this paper.

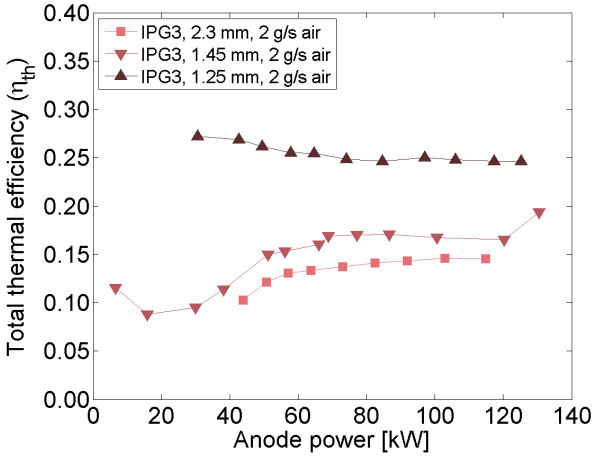

Figure 13: Total thermal efficiency for air (adapted from [10])

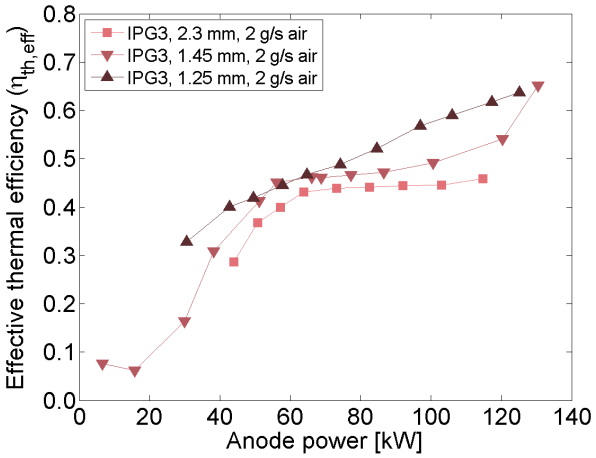

Figure 14: Effective thermal efficiency for air (adapted from [10])

Continuing to display discrepancies from its pure counterpart, the Ar:N_2 flow maintains a marginally decreasing total thermal efficiency above the asymptote of 20%, with minimal variation between chamber thicknesses. However, the effective efficiency shows that usable thermal power within the flow is steadily increasing, with a clear preference for the thinner chamber walls. These results again show good agreement with results for air (Figures 13 and 14), with the impact of reducing

wall thicknesses clear.

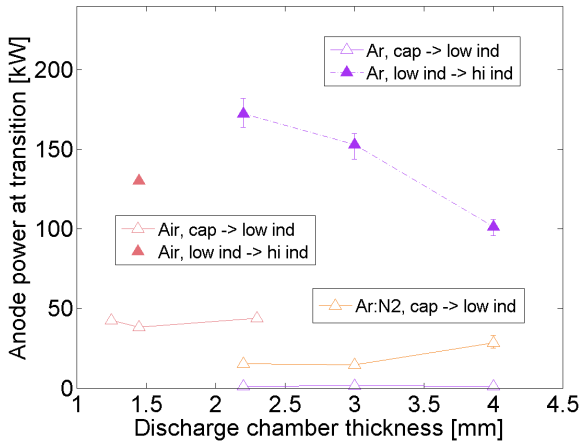

Figure 15: Discharge transition input powers for varying gases and wall thicknesses

The gradients of thermal power and efficiency in Figures 7 - 14 are directly dependent on the discharge regime exhibited by the IPG. An analysis of the input electrical power required for each transition with respect to the varying wall thicknesses is thus displayed in Figure 15.

Transitions are separated into two distinct categories. The first is a transition from the capacitive mode to the first or "low" inductive mode, as discussed previously in Section 2. However, inductive plasma generators can support a number of stable (and unstable) inductive discharges [11], thus defining the second category as transitions between low inductive and high inductive operation.

Transitions to the low inductive mode for argon occur at very low input powers ($\approx$ 1 kW), at a point where fluctuations in the power supply current and potential make precise measurements difficult. However, transitions to the high inductive regime show clear results, with a substantial decrease in power required for greater wall thicknesses. The magnitude of these decreases is far greater than that of geometric-dependant factors such as the discharge chamber pressure or surface to volume ratio and hence these factors may be neglected for this analysis.
Results for Ar:N_2 show the increasing power required to transition into the first inductive regime for increasing dielectric separation. These results are much clearer than their pure argon counterpart as the addition of nitrogen to the flow requires greater input power to overcome pre-ionisation processes such as dissociation and the distribution of energy into the rotational and vibrational energy modes. In all three conditions, none achieved sufficient power coupling to instigate a transition to the higher inductive mode. However, this transition was not expected in the conditions chosen and usually requires a higher operating frequency as well as mechanical nozzle to increase chamber pressure.
Comparisons with the air conditions display similarities to Ar:N_2, with transitions occurring again at elevated input powers due to the wholly diatomic nature of the propellant and thus a greater quantity of particles required to transition through other modes of energy before achieving ionisation. Curiously though, while the thinnest wall condition of 1.25 mm yielded the greatest jet thermal power and total thermal efficiency, it was not able to transition to the higher inductive regime as the 1.45 mm condition had. As a result, the 1.45 mm configuration displayed the greatest effective thermal efficiency owing to the inherent decrease in chamber cooling power once the higher inductive "pinching" mode is reached [6]. A possible theory to explain why further decreases in the discharge wall thickness did not continue to improve performance is detailed in Section 5.

5. DISCUSSION

Given the discrepancy in results gathered from this investigation as well others previously, a theory is required to reconcile the inconsistent behaviour relating to variations of wall thickness within inductive discharges. Firstly, pure argon operation displays an inverse behaviour to air and Ar:N_2 flows, with higher thermal power measured when implementing thicker discharge chamber walls. Secondly, past a given value within the air investigation campaign, further reductions in the chamber wall thickness produced higher thermal powers but failed to facilitate a transition to the higher inductive mode. In order to reconcile these differences, the influences of both electromagnetic and thermodynamic behaviour within the discharge chamber must be considered.

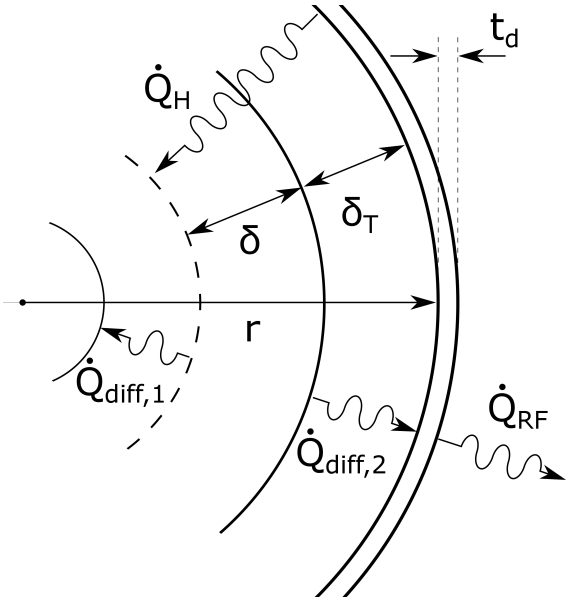

Figure 16: Thermodynamic and electromagnetic behaviour within the inductive discharge

Increasing the chamber wall thickness acts to decrease the net magnetic field strength to which charged particles within the plasma are exposed, as discussed previously in Section 3. However, this statement is true for all dielectric or non-conductive media, thus requiring consideration of the thermodynamic relationship between the discharge chamber wall and the thermal boundary layer. Consider the inductive discharge cross-section seen in Figure 16, where $\dot{Q}_H$ is the heat flux generated from the externally-applied coil magnetic field and $\dot{Q}_{diff,1}$ and $\dot{Q}_{diff,2}$ are the diffusion of thermal power radially inwards and outwards from the skin depth respectively.

As the wall thickness is decreased, the thermal energy used to establish the skin depth should increase owing to the greater net magnetic field strength incident on the plasma. However, decreasing the tube wall also reduces the time taken for a given quantity of thermal energy to traverse the chamber wall and reach to cooling water flow on the other side. As a result, energy flows more freely through the discharge tube wall and a lower accumulation from $\dot{Q}_{diff,2}$ would in turn produce a lower internal wall temperature. Discharges within this system are of a relatively high pressure (1000 - 3000 Pa), relying on collisions to distribute energy within the flow. Hence a lower discharge chamber wall temperature would in theory provide a lower baseline energy for near-wall particles and extract more energy from the skin depth. As a result, the thermal boundary layer should increase, assuming that the effect of lowering the chamber wall temperature dominates that of supplying more energy to the flow through the increased incident magnetic field strength.

If the thermal boundary layer is treated as a zone of negligible ionisation degree owing to the low local energy, then the thickness of the boundary layer may also be considered a dielectric separation between coil and plasma. This is an important assumption given that, as seen in Figure 1, electric fields across the coil surface and those generated within the plasma (particularly those used to form the skin depth) act in opposing directions. Therefore any dielectric medium separating the two fields will have an influence on the magnitude of the resultant azimuthal field within the plasma and the Coulombic interaction between charged species with opposing trajectories. The assumption of such behaviour within the discharge may be used to explain the results discussed previously.

The first case considers the pure argon discharge. As can be observed in Figure 10, thermal boundary layers for argon are much smaller than those involving nitrogen. This is due to argon's inability to store energy in modes other than excitation and ionisation, as opposed to diatomic molecules' additional processes of rotation, vibration, and dissociation. As a result, the primary dielectric separation in this discharge is produced by the discharge chamber wall and the net magnetic field strength remains high due to charged particle proximity to the coil surface. This would explain the observed behaviour, with the increase in wall thickness acting primarily to separate the opposing electric (and magnetic) fields while the degree of ionisation in the skin depth region remains high due to a small thermal boundary layer and hence high net magnetic field strength.

The second case considers the trend of non-monatomic flows (Ar:N_2 and air) and their preference of thinner walls up to a given point, beyond which discharge transitions are hindered rather than assisted. In these situations, the theory discussed previously would account for thinner walls

providing greater energy coupling by increasing the separation between charged species within the plasma and on the coil surface. This approach would also provide a possible explanation for the thinnest condition (1.25 mm) being unable to facilitate a transition to the higher inductive mode, with the increased thermal boundary layer crossing some point beyond which the net magnetic field strength incident on the flow was inadequately paired with the gas inflow conditions. This hypothesis will form the basis of future measurement campaigns which will focus on the magnetic field distribution across the discharge cross-section.

It is therefore recommended that investigations considering the impact of dielectric separation within inductive plasma discharges consider not only mechanical separations from component geometry, but also gasdynamic separations generated within the discharge volume itself.

This consideration is of particular importance when determining the desired propellant configuration for a particular mission. As seen through the results in this paper, mixtures of dissimilar gases can exhibit strong characteristics of a minority constituent, with strong implications on system performance for a given thruster geometry. As a result propellants and thruster components may be chosen to take advantage of favourable performance of a particular gas or the availability of a particular resource. In the context of space operations, this may correlate to long-range, multi-destination missions, or those centred around a propellant supply of varying/cyclic chemical composition. The ability to react to such changes in the operational environment, or tailor a mission simply by supplying an existing propulsion system with a particular propellant mixture, is an example of IEP's inherent flexibility and potential for future space operations.

6. CONCLUSION

This paper has investigated not only the influence of dielectric separation within inductive plasma discharges, but also what may be considered as a dielectric medium in and around the discharge volume. Results from argon plasmas show a preference for thicker tubes, with the necessary power to transition to the higher inductive mode decreasing with increasing wall thickness. Results for $Ar:N_2$, as well as previous investigations for air, show a preference towards thinner tubes, with significant increases in the effective thermal efficiency of the system observed with thinner walls. This behaviour continues up until some critical point, beyond which thermal energy is still produced in greater magnitude but transitions to the higher inductive mode are not observed. It is proposed that this behaviour stems from the thermal boundary layer within the inductive discharge behaving as an additional dielectric separation, adding to that of the discharge chamber wall thickness. The chamber wall thickness therefore directly and indirectly affects the net magnetic field strength incident on charged particles, partially by containment within the chamber dielectric material as well as by increasing or decreasing the thermal boundary layer by means of the time taken for thermal energy to travel through the chamber walls into the external cooling water flow.

ACKNOWLEDGEMENTS

This paper would like to acknowledge contributions made by both the Sir Ross and Sir Keith Smith Fund (the Fund) and the German Research Foundation (DFG). The Fund supplies funding for personnel within this project, while DFG contributes funding for experimental costs and equipment under Project HE 4563/3-1.

References

[1] Gerstenmaier, W., "Exploration Strategy Update to NAC," www.nasa.gov/sites/default/files/atoms/files/gerst-april-2015.pdf, April 2015.

[2] Parissenti, G., Koch, N., Pavarin, D., Ahedo, E., Katsonis, K., Scortecci, F., and Pessana, M., "Non-conventional Propellants for Electric Propulsion," *Presented at Space Propulsion 2010*, San Sebastian, Spain, May 2010.

[3] Shabshelowitz, A., *Study of RF Plasma Technology Applied to Air-Breathing Electric*

Propulsion, Ph.D. thesis, University of Michigan, 2013.

[4] Cifali, G., Misuri, T., Rossetti, P., Andrenucci, M., Valentian, D., Feili, D., and Lotz, B., "Experimental Characterization of HET and RIT with Atmospheric Propellants," *32nd International Electric Propulsion Conference*, September 2011, IEPC-2011-224.

[5] Schoenherr, T., Kmourasaki, K., Romano, F., Massuti-Ballester, B., and Herdrich, G., "Analysis of Atmosphere-Breathing Electric Propulsion," *IEEE Transactions on Plasma Science*, Vol. 43, No. 1, January 2015, pp. 287 – 294.

[6] Herdrich, G. and Petkow, D., "High-enthalpy, water-cooled and thin-walled ICP sources: characterization and MHD optimization," *Journal of Plasma Physics*, Vol. 74, No. 3, 2008, pp. 391 – 429.

[7] Abdel-Rahman, M., von der Gathen, V. S., and Gans, T., "Transition phenomena in a radio-frequency inductively coupled plasma," *Journal of Physics D: Applied Physics*, Vol. 40, No. 1678-1683, 2007.

[8] Hopwood, J., "Review of inductively coupled plasmas for plasma processing," *Plasma Sources Science and Technology*, Vol. 1, 1992, pp. 109–116.

[9] Kortshagen, U., Gibson, N. D., and Lawler, J. E., "On the E-H mode transition in RF inductive discharges," *Journal of Physics D: Applied Physics*, Vol. 29, 1996, pp. 1224–1236.

[10] Nawaz, A. and Herdrich, G., "Impact of Plasma Tube Wall Thickness on Power Coupling in ICP Sources," *Plasma Sources Science and Technology*, Vol. 18, 2009.

[11] Lieberman, M. and Lichtenberg, A., *Principles of Plasma Discharges and Materials Processing*, John Wiley and Sons, Inc, Hoboken, New Jersey, 2nd ed., 2005.